J. Membrane Biol. 3, 313–334 (1970)

Volume Flows and Pressure Changes During an Action Potential in Cells of *Chara australis*

I. Experimental Results

PETER H. BARRY*

Biophysics Laboratory, School of Biological Sciences, Flinders University, Bedford Park, South Australia, 5042 and Department of Physiology, School of Medicine, Center for the Health Sciences, University of California, Los Angeles, California 90024

Received 20 May 1970

Summary. Methods have been used for monitoring either volume flows or pressure changes, simultaneously with membrane potentials, in giant algal cells of *Chara australis* during an action potential. The volume flows were measured from the movement of a mercury bead in a capillary tube recorded by a photo-transducer. The pressure changes were measured by monitoring the deflection of a thin wedge, resting transversely across a cell, and using the same photo-transducer, the deflection of the wedge being directly related to the cell's turgor pressure. The average maximum rate of volume flow per unit area during an action potential was 0.88 ± 0.11 nliter $\cdot$ sec^{-1} $\cdot$ cm^{-2} in the direction of an outflow from the cell (total volume outflow being about 3 nliter $\cdot$ cm^{-2} per action potential). Similarly, the maximum rate of change of pressure was $19.6 \pm 3.8 \times 10^{-3}$ atm $\cdot$ sec^{-1} (peak change being $19.3 \pm 2.9 \times 10^{-3}$ atm equivalent to 14.7 ± 2.2 mm Hg). The volume flow and pressure changes followed the vacuolar potential quite closely, the peak rate of volume flow lagging behind the peak of the action potential by 0.17 ± 0.08 sec and the peak rate of pressure change leading it by 0.09 ± 0.07 sec.

Teorell (1958) and Kobatake and Fujita (1964*a*, *b*) have proposed various electro-kinetic models to explain the mechanism of membrane excitability in nerve, whereas Teorell (1961) in particular has proposed that electro-osmosis might also play a role in the action potential of the giant algal cell *Nitella*. Teorell, for example, suggests that as a stimulating current passes through a membrane it will cause an electro-osmotic flow which in turn increases the membrane resistance and the potential drop by changing the ion concentration profiles in the membranes. This change in the potential

* Present address: Physiological Laboratory, Downing Street, Cambridge, CB2 3EG, England.

difference (p.d.) will, he suggests, then increase the electro-osmotic flow The process would continue to increase the flow were it not for the increase in hydrostatic pressure caused by the flow itself which eventually tends to balance the electro-osmotic flow and to cause the whole system to revert back to its original equilibrium. Since each of the models predicts that volume flows and pressure changes should accompany action potentials, it is of interest to observe and measure such changes during excitation. This will be the subject matter of this and the accompanying paper. This paper will deal with experimental measurements of both volume flows and pressure changes, and the second paper (Barry, 1970, which will from now on be referred to as paper II) with a theoretical analysis of these changes.

The giant algal cells of *Chara australis* proved to be an extremely convenient preparation for such measurements for a number of reasons: they are large rigid cylindrical cells; they have slow 2 to 3-sec duration action potentials; and they have a large hydrostatic pressure difference between the inside of the cells and the external solution, generally about 6 to 8 atm.

The volume flows were measured for cells held centrally with silicone grease in a split stopper between two chambers as indicated in Fig. 1. The volume flow measured, integral of the rate of volume flow, is the total volume of both water and solutes that have passed into the cell at one end and out of the cell at the other. The cells were normally stimulated at one end, and the resulting action potential would be expected to cause a volume outflow at that end. This would tend to cause a drop in the cell's turgor pressure (the hydrostatic pressure resulting from the elastic distension of the cell and balancing the difference in osmotic pressure between the inside and outside solutions) and a resultant inflow of water from the other end of the cell. When one end of the cell is stimulated, the resulting action potential may or may not be transmitted through the split-stopper to the other end of the cell, depending on the effectiveness of the silicone-grease seal around the cell at the stopper. When an action potential is thus transmitted, the sequence of events might be as follows: initially the rate of volume flow dV/dt would be expected to follow the first action potential, decaying to zero after its completion, and then as the action potential passes to the other end of the cell the rate of volume flow should reverse. The volume flow would thus be expected to rise slowly to a maximum as one end of the cell is excited and to revert slowly back to its original value as the action potential reaches the other end and causes an outflow at that end. If the action potential is not transmitted, the rate of volume flow will only have the action potential at one end to follow so that the volume flow would thus be expected to rise slowly to a maximum and then to remain constant.

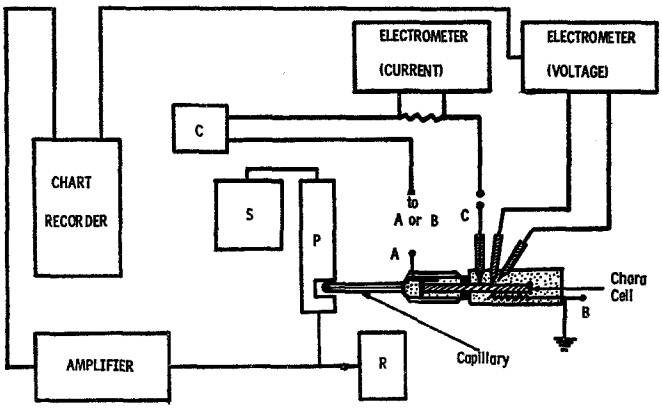

Fig. 1. A schematic diagram of the experimental arrangement used to measure water (volume) flows in cells of *Chara australis* during action potentials. The diagram is similar to that shown in Fig. 1 of Barry and Hope (1969), and the equipment is identical with that shown in both Figs. 1 and 2 of that paper except that in the experiments in this paper, where short transients flows were measured, it was not necessary to enclose the double-walled Pyrex chamber in an additional thermal reservoir. In the schematic blocks, *C* refers to the current generator, *P* to the photo-transducer optical bench, *S* to the four-transistor stabilized voltage supply for the light source and *R* to the resetting or backing-off circuit (with its own stabilized battery supply) for the amplifier. The terminals *A*, *B* and *C* are connected to Ag/AgCl electrodes, with *C* being in an internal (vacuolar) KCl-filled glass microelectrode. The two potential-measuring glass microelectrodes were also KCl-filled and were connected to the electrometer via calomel half-cells (not shown)

The turgor pressure of the cells was ascertained by measuring the deflection of a thin wedge resting transversely across a cylindrical cell (Figs. 2 & 3). It will be shown that the magnitude of the deflection can be directly related to the radius and turgor pressure of the cells. For these experiments, the whole cell was in the same bath and completely surrounded by solution. It is to be expected that if there is a volume outflow from these fairly inelastic plant cells during excitation this will cause a small drop in turgor pressure which could be measured with the continuous monitoring procedure just mentioned.

Materials and Methods

The cells used for measuring volume flows were mature internodal cells of the giant algae *Chara australis* obtained from Camden (New South Wales, Australia). These were single cylindrical cells of length 6.2 to 10.3 cm and of diameter 1.14 to 1.35 mm. The cells used for measuring pressure changes were of the same species but included some cells from cultured stocks of both Camden and Tasmanian origin. These cells included both internodal and whorl cells and varied in length from about 1.76 to 6.7 cm and in diameter from about 0.88 to 1.32 mm. The coding used in this paper to

refer to each action potential measurement is as follows. The first number and letter refer to the particular cell and the next number to the action potential; e.g., 2M-15, refers to the 15th action potential for cell 2M. Artificial pond water (A.P.W.) solutions contained NaCl (1.0 mM), KCl (0.1 mM) and $CaCl_2$ (varying from 0 to 0.5 mM). The concentration of $CaCl_2$ is indicated in parenthesis [e.g., A.P.W. (0.5) indicates a concentration of 0.5 mM $CaCl_2$] and was changed in order to try and modify the shape of the action potential.

The errors quoted in the Results section of this paper are the standard errors of the means.

Volume Flow Measurement

The overall experimental arrangement for measuring these volume flows is shown schematically in Fig. 1. A detailed description of the equipment has already been given and illustrated (Barry, 1967; Barry & Hope, 1969, e.g., Figs. 1 & 2). Briefly, the cell was held firmly with silicone grease in a Perspex split-stopper. One half of the cell was in an open chamber, attached to the fixed microscope stage of a binocular microscope and was accessible for electrode insertion. The other half was in a closed double-walled Pyrex chamber connected to a thick-walled capillary tube (bore 1.36 mm). A small bead of mercury, 2 to 5 mm in length, supported in equilibrium by the column of solution, then obstructed a light beam, falling on a silicone solar cell element. The light source was fed from a stabilized *d-c* supply, and the output of the solar cell amplified through a current amplifier and displayed on a two-channel chart recorder (response time, 0.12 sec). Thus the fraction of the beam (full width about 1.3 mm) falling on the solar cell was proportional to changes in volume in the closed chamber (i.e., the volume of solution transported transcellularly by the cell). The photo-transducer output was backed-off by a 110-step stabilized resetting circuit to allow a maximum overall sensitivity for the whole transducer arrangement of about 1 mamp $\cdot$ nliter^{-1} (full scale deflection = 10 mamp) over a range of about 1 to 2 μliters. Glass microelectrodes (tips 5 to 15 μ) filled with 3N KCl and calomel half-cells were used together with Keithley 603 electrometers for measuring membrane p.d.'s. Stimulating currents (2 to 13 μamp $\cdot$ cm^{-2}) were passed in one of three ways: between the two external Ag/AgCl electrodes (*A* and *B* in Fig. 1) at either end of the cell; or between a Ag/AgCl wire in a KCl-filled glass electrode (*C* in Fig. 1) and either the external Ag/AgCl electrode A at the closed chamber or electrode B at the open chamber. Thus either end of the cell could be stimulated initially.

Hydrodynamic analysis has shown that the time taken for the movement of the mercury drop to reach a maximum is less than about 1 msec. Since the time constant of the electronics was negligible (i.e., <20 μsec), the limiting factor for absolute measurements of flows was the time constant of each chart recorder channel, i.e., about 0.1 sec. However, time delays between the voltage trace and the associated volume flows could be estimated within the error of pen synchronization (about 0.02 sec.). This was checked during each experiment from the transition in trace width and slope for each channel at the change from slow to fast chart recorder speeds. The errors in the absolute values of the volume flow are less than about $\pm 5\%$ and are caused by errors in chart reading and amplifier calibration.

Turgor Pressure Measurement

The turgor pressure (or hydrostatic pressure exerted by the cell wall) of cylindrical plant cells was ascertained by measuring the deflection of a thin wedge resting transversely across a cell as illustrated in Figs. 2 and 3. In essence, the principle is similar to

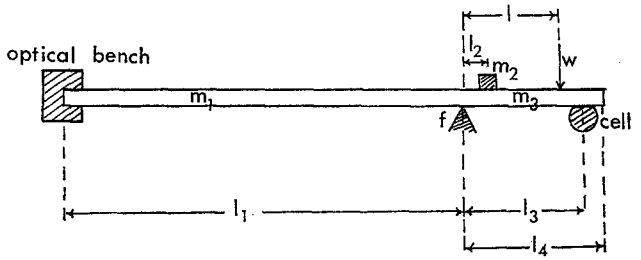

Fig. 2. A schematic diagram of the pressure transducer setup showing the essential geometry of the system. m_1, m_3 and m_2 represent the masses of the lever arms and counterbalance, respectively. W (M in the text) represents the position of the weight, and f the fulcrum. The lengths and masses are as follows $\ell_1 = 23.3$ cm, $\ell_2 = 2.7$ cm, $\ell_3 = 5.3$ cm, $\ell_4 = 5.6$ cm, $m_1 = 4.6$ g, $m_2 = 14.8$ g, $m_3 = 2.5$ g

that used by Tazawa (1957) for measuring cell turgor pressure. The relationship between the turgor pressure P, the deflection X of the wedge below the normal cell surface, and the radius of the cell a was derived theoretically for a thin wedge. An outline of the method of derivation is given in Appendix A and full details in a Ph. D. thesis (Barry, 1967). The relationship is that

$$P = \pi - \pi_0 = \alpha \frac{Mg}{aX} \tag{1}$$

where P is the turgor pressure of the cell; π and π_0 are the osmotic pressures of the external solution and the cell sap, respectively (σ, the reflection coefficient in both cases is taken to be 1.0); M is the mass on the wedge; g is the acceleration due to gravity; a is the radius of the cell; and X is the deflection of the wedge. α is a dimensionless constant calculated to be $\simeq 0.4$. Justification for Eq. (1), however, does not rely merely on theoretical grounds; as will be discussed later in this section, the relationship was verified experimentally. By differentiating Eq. (1), it may be shown that for small changes in pressure ΔP (i.e. $\lesssim 1\%$), the change in deflection ΔX may be shown to be given by:

$$\Delta X = -\frac{X}{P} \Delta P \tag{2}$$

where X and P are the absolute values of the deflection of the wedge resting on the cell wall and the turgor pressure of the cell, and, as will be discussed, whose ratio may be determined from a simple calibration curve. The apparatus used to measure such deflections is shown in Figs. 2 and 3. In practice a stainless-steel razor-blade edge (appropriately blunted and resharpened) was used as the thin wedge. It was connected with Araldite to the short end of a lever arm. The lever arm (lever ratio approximately 4.2) used to amplify this deflection was made of light aluminium U-shaped in cross-section for strength and rigidity. The long arm weighed about 4.6 g, and there was a fixed counter-balance of about 14.8 g on the shorter arm to keep the lever in equilibrium when there was no weight on the wedge.

The deflection of the end of this long lever was measured by allowing it to obstruct partially the light beam used in the photo-transducer arrangement already discussed briefly in this paper and at length by Barry (1967) and Barry and Hope (1969) for measurements of volume flows. Again the amount of unobstructed light falling on the

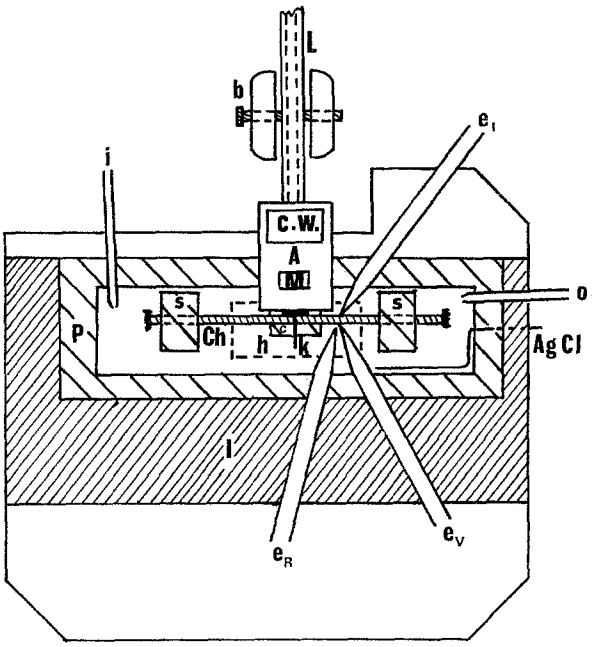

Fig. 3. A schematic diagram of the cell holder and part of the pressure transducer used for measuring pressure changes in a cell during an action potential. The *Chara* cell, *Ch*, was placed in a Perspex bath (internal length 12 cm) *P*. This Perspex bath was in turn clamped to an iron plate *I* with a hole *H* for illumination of the cell through it. The cell was held at either end in two Perspex stocks with its center resting on a central platform *C*. A knife edge *K* resting across the cell was connected to an aluminium tray *A* at the short end (5.3 cm) of the lever *L* which pivoted on either 'round' or 'knife-edged' iron bearings *b*. The torque owing to the long arm (23.3 cm) was balanced by the counterweight *C.W.* Masses *M* could be placed on the aluminium tray, and their effective weight at the knife edge caused a deflection of the cell surface, which was related to the turgor pressure of the cell. This deflection was amplified by the lever system, the tip of the long lever obstructing the light beam of the photo-transducer shown in Fig. 1 and in Figs. 1 and 2 of Barry and Hope (1969). e_1 and AgCl (for KCl and Ag/AgCl electrodes, respectively) were current electrodes used for stimulating the cell. e_R (reference) and e_V (vacuolar) were again KCl-filled glass microelectrodes used for monitoring the membrane p. d., E_{V0}. *i* and *o* were inlet tube and outlet tube, respectively, used for changing the solution in the bath

solar cell element was measured. This area of the light beam *A* exposed by a rotation of the lever arm is directly related to the deflection of the thin wedge *X* by

$$A = \frac{\ell_1}{\ell_3} b X$$

where *b* is the width of the slit and ℓ_1 and ℓ_3 are shown in Fig. 2.

The whole cell holder and the lever arrangement were rigidly attached to the optical bench to reduce relative movement of the two. Also, a heavy iron block clamped to the Perspex bath added extra weight to the apparatus to reduce relative vibrations in it.

The bearings, used for the lever movement, consisted of a small cylindrical iron rod passing through two holes of a slightly larger diameter in the lever arm. This had two bearing surfaces, one cylindrical and the other knife-edged so that by merely rotating the rod the bearing surfaces could be changed from one type to the other. This will be further discussed in relationship to the time response of the pressure transducer in Appendix B. Microelectrodes were inserted into the cells with micromanipulators, and again the associated electronics was the same as previously described. As before, there was also an external Ag/AgCl electrode fixed to the Perspex cell holder (*see* Fig. 3).

The plant cells were viewed with a microscope; a slot in the iron block and an aluminum mirror provided transmitted light illumination. The cell was irrigated with bathing solution from the top (as in Fig. 3), the level being controlled by vertical adjustment of a siphon tube through which water was extracted by an electric pump into a glass reservoir below the electrostatically shielded cage. Those cells longer than about 5 cm were held firmly with both ends in Perspex stocks, whereas the smaller ones were attached directly to each stock by a piece of silk thread attached to their nodes. Most of the cells were also held down against the central platform by two elastically tensioned plastic-covered wires in order to reduce the zero error in some of the measurements caused either by the cells not lying flat on the platform or by their tendency to bend slightly as the initial weight was placed on the wedge. Measurements of the deflections of the thin wedge were made for different effective masses on the wedge (the actual effective weight being corrected for the fact that the mass was not immediately above the cell, as indicated in Figs. 2 & 3). As predicted by Eq. (1), the deflection X was linearly proportional to the effective mass on the wedge for masses varying from 1.33 to 6.77 g.

The deflection X was also measured as a function of the osmotic pressure of the external solution. The normal solution used was A.P.W. (0.1) with 25, 50, 100 and 150 mM sucrose (with osmotic pressures varying from about 0.66 to 3.97 atm at about 20 °C). The results of such calibration experiments are shown in Fig. 4 for one cell, where it is shown that π is inversely proportional to X, as expected from the theoretical equation

$$\pi = \pi_0 - \alpha \frac{Mg}{aX}. \tag{3}$$

The experimental scatter seen in Fig. 4 and in all of the other calibration curves was within the experimental errors expected, and the variations from the theoretical curves were random when $\pi - \pi_0$ was not too small. The intercept of the line of best fit with the osmotic pressure axis then gives an estimate of the osmotic pressure of the cell sap π_0 which equals the turgor pressure of the cell in a simple A.P.W. solution without sucrose. This together with the deflection of the wedge in such a solution then allows an evaluation of the calibration factor P/X used in Eq. (2). For example, in Fig. 4 both curves for effective masses of 1.33 and 2.71 g intercept the ordinate at approximately 6.2 atm, which therefore is an estimate of the turgor pressure of the cell. Table 2 shows that, with the exception of cells 6F and 6M, the experimental values of α are satisfactorily close to the predicted values, considering the approximate nature of the assumed cell deformation in the theory. It should of course be emphasized that the calibration factors are absolutely empirical and are not dependent on the absolute reliability of the theoretical analysis.

Because of high-frequency noise at the output of the pressure amplifier, caused by artifactual vibrations of the pressure transducer arm, a condenser, acting as a low-pass filter, was placed across the terminals of one of the galvanometric chart recorder channels. Since the recorder, which was fed from a current source output from the amplifier system, had a resistance of 3 $K\Omega$ and the filter a capacity of 90 μF, the time constant of this recording circuit was 0.27 sec. Thus any signal with a frequency less than about

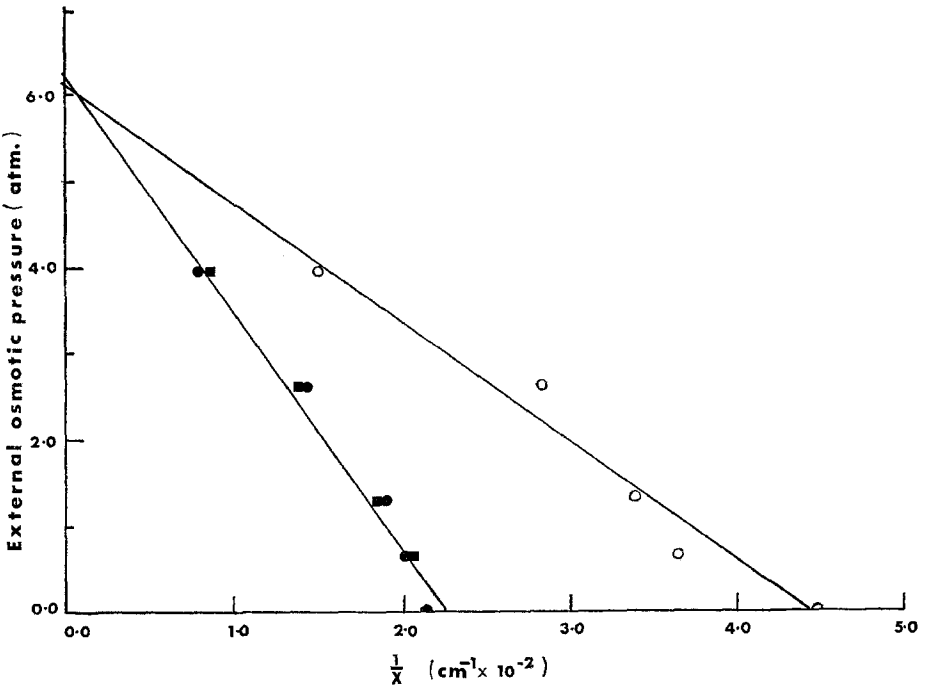

Fig. 4. The calibration curve of the osmotic pressure of the external solution, π (atm), plotted as a function of the reciprocal of the deflection of a knife edge, 1/X ($cm^{-1} \cdot 10^{-2}$), on a cell of *Chara australis* (cell J) in a solution of A.P.W. (1.0). As discussed in the text, the calibration curves are plotted for two different weights on the cell. The values of curve *I*, with points marked ∘, were measured on the first day for $M=1.33$ g. The values for curve *II*, with points marked • and ▪, were measured on the second day for $M=2.71$ g from two sets of experimental runs. Each set of values was the mean of two sets and the standard error of this mean in each case was less than about 3 %. The constant α was 0.47 and 0.46 for curves *I* and *II*, respectively. The intercept on the pressure axis cut by each curve represents the turgor pressure of the cell [see Eq. (1)]

0.1 sec^{-1} would be transmitted only slightly diminished in magnitude, but retarded by about 0.27 sec. The effect of this low-pass filter is discussed in more detail in paper II where it is calculated for typical action potential frequencies.

The theoretical response of the transducer arrangement was investigated, and it was calculated (Barry, 1967) that for pressure changes occurring in times greater than about 10 msec, the moment of inertia of the measuring system has a negligible effect on the time course of the deflection. This is supported by the experimental evidence discussed in Appendix B, where both extra inertia and the increased area of bearing surfaces do not cause any significant increase in the time delays.

For these action potential measurements, the cells were stimulated at one end between an internal KCl-filled glass microelectrode and an external Ag/AgCl one. The overall membrane p.d. (vacuole-external solution) was measured with two KCl-filled glass microelectrodes, the vacuolar one being placed opposite the internal current electrode as shown in Fig. 3. The cells were usually stimulated at intervals of about 10 min.

The pressure transducer was normally calibrated at the beginning of the experiment, as already described. In the case of cell 6N, it was also calibrated at the end of the first day, and for cells 6J and 6K again on the second day. These three experiments were continued for two days, and there was no significant change in the pressure or calibration factor between calibrations (e.g., Fig. 4).

As already mentioned for volume flow measurements, pen synchronization errors were generally $\lesssim 0.02$ sec. The estimated errors in the absolute magnitude of the pressure change are less than about $\pm 10\%$ ($\pm 5\%$ for calibration and $\pm 5\%$ amplifier gain and for errors in chart measurement). The estimated errors for the relative magnitudes of the rate of change of pressure are less than about 5%.

Results

Volume Flows

There is a volume flow during an action potential in *Chara*[1] which corresponds to an outflow of solute and water from the cell interior to the external solution. Now, as already mentioned, only one end of the cell was stimulated at one time by electrode pairs A–C or B–C, and it was noted that certain cells did not usually propagate an action potential through the split-stopper. As expected for these cells, the volume of fluid (water + solute) ΔV flowing through the cell increased to a maximum and stayed constant (as shown in Fig. 5) when that end of the cell in the open chamber

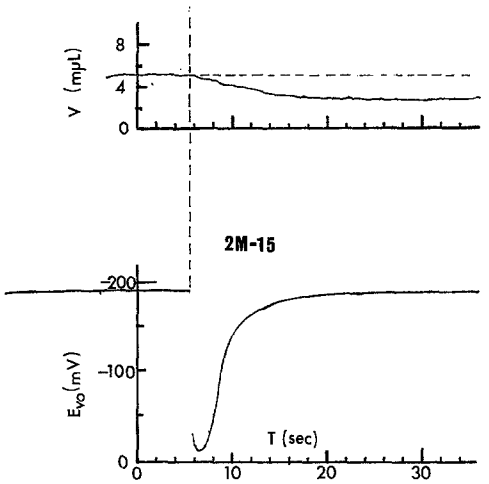

Fig. 5. Fast recording of the typical changes in volume V(nliter) and membrane p.d. at end B, E_{V0}, during an action potential for a cell of *Chara australis* (cell 2M-15) held in a transcellular arrangement in a solution of A.P.W. (1.0). The open end B was stimulated directly. In this case, there is only a monophasic flow corresponding to a volume outflow at end B, as this was one of the cells which was not transmitting action potentials properly through the Perspex stopper

1 Preliminary measurements of such volume flows were reported by the author in 1965 at the Conference on the Physiology of Giant Algal Cells, in Canberra, Australia.

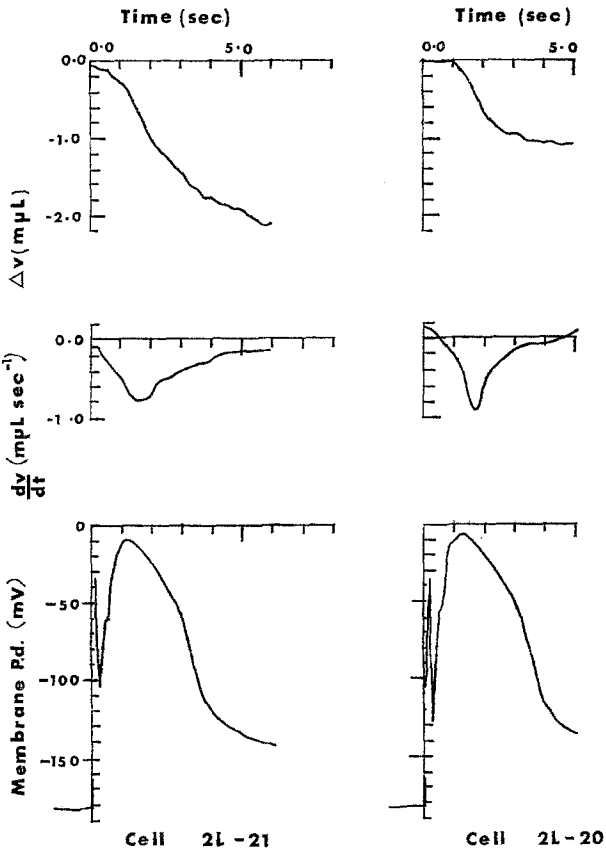

Fig. 6. Typical changes in volume, ΔV (nliter), rate of volume flow, dV/dt (nliter·sec^{-1}) and membrane p.d., E_{V0}, during an action potential for cells of *Chara australis*. The points on these curves were measured and replotted from chart recordings similar to those shown in Fig. 5. Cell 2L was kept in a solution of A.P.W. (1.0). In both experimental runs, the action potentials were stimulated and recorded at end B and the negative sign of the change in volume and the volume flow implies an outflow at end B

(referred to in future as B) was stimulated with external electrode pair B–C (Fig. 1). This implies that the rate of volume flow dV/dt increases to a maximum as the action potential reaches a maximum so that there is a net loss of volume during excitation. This is clearly shown in Fig. 6 for two action potentials on the same cell.

Most cells, however, did propagate action potentials. This is shown clearly in Fig. 7 where, as in all cases, it must be remembered that the membrane p.d. being measured is the one at end B. In this record, the end of the cell in the closed chamber (referred to in future as A) was stimulated. Initially there was just an artifact in the p.d. at end B, while the action

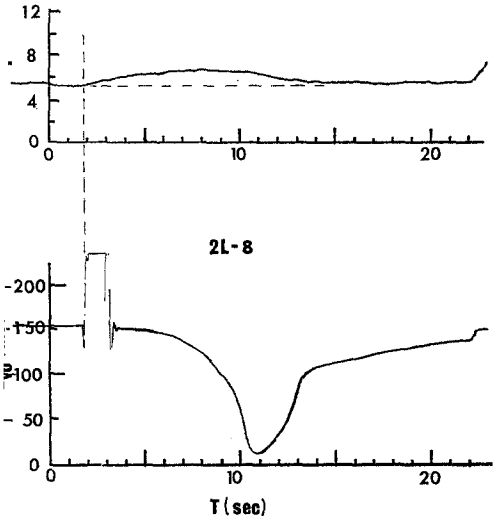

Fig. 7

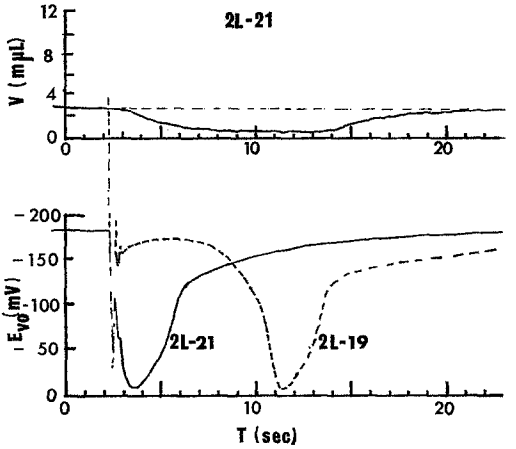

Fig. 8

Fig. 7. Fast recording of the typical changes in volume V(nliter) and membrane p.d. at end B, E_{V0}, during an action potential for a cell of *Chara australis* (cell run 2L-8) held in a transcellular experimental arrangement in a solution of A.P.W. (1.0). End A was stimulated initially. This shows the situation in which an action potential was transmitted from end A to end B along the stopper (velocity in stopper $\simeq 0.12$ cm · sec^{-1}) with an initial volume outflow at end A. The initial square pulse is a current stimulus artifact

Fig. 8. Fast recording of typical changes in volume V (nliter) and membrane p.d. at end B (E_{V0} refers to the potential of the vacuole with respect to the external solution), during an action potential for a cell of *Chara australis* (cell run 2L-21 with a reconstruction of run 2L-19) held in a transcellular experimental arrangement in a solution of A.P.W. (1.0). The open end of the cell B was stimulated directly with a current pulse. This recording shows a typical biphasic volume flow resulting from the action potential being transmitted from end B to end A. The p.d., E_{V0}, was measured at end B of the cell, which was the end initially stimulated. At first there was a volume outflow at end B of the cell following the action potential at that end. Then, after a few seconds, a flow began in the opposite direction corresponding to the action potential having reached end A and caused a volume flow in the reverse direction. The transmitted action potential (*see* also Fig. 7), has been simulated by superimposing the recording for run 2L-19, in which end A had been stimulated initially in order to show the combined effect of action potentials at both ends of the cell

potential was stimulated at end A, and a volume flow of water corresponding to an outflow of fluid at end A caused by the action potential. The net volume of fluid flowing through the cell then reached a steady level (i.e., the rate of flow decreased to zero), remained there for a while and then, in association with a transmitted action potential, the net volume of fluid flowing returned to its original base level (i.e., the rate of flow was now in the reverse direction), corresponding to an outflow of fluid at end B. The

Table 1. *Volume flow, volume flow rate, and correlation of the time course o*

Exp.	No. of action potentials used	$\bar{\ell}$ [a] (cm)	$2a$ [b] (cm)	Time constants (sec)	
				τ_{ap} [c]	$\tau_v - \tau_{ap}$ [d]
M	6	5.15	0.135	1.03 ± 0.06 [f]	-0.03 ± 0.12
$2L$	12	4.15	0.131	0.78 ± 0.14	$+0.18 \pm 0.04$(11)
$2M$	7	2.6	0.118	1.06 ± 0.06	$+0.35 \pm 0.15$(6)
$2N$	4	3.95	0.136	1.09 ± 0.13	$+0.18 \pm 0.17$
Average values of parameters [g]					$+0.17 \pm 0.08$

[a] $\bar{\ell}$ = average length of each end of cell.

[b] a = cell radius.

[c] τ_{ap} = time to peak of action potential, corrected for chart recorder delays.

[d] $\tau_v - \tau_{ap}$ = difference between the time to the peak volume flow rate and to the peak of the action potential, corrected for chart recorder delays.

composite picture is shown approximately in Fig. 8 where the solid lines indicate the net volume flow through cell 2L associated with action potential 21 which had initially been stimulated at end B. The trace for the action potential at end A during this time was assumed to be somewhat similar to that measured earlier for action potential 19 when end A was stimulated initially. This trace (dashed line) was then superimposed on the former recording. Although there is a slight discrepancy in the time delay of the projected transmitted pulse, this clearly shows the role of the action potentials at either end of the cell in causing the rate of volume flow to increase to a maximum and to decay to zero during the action potential at one end of the cell and then to reverse, increasing to a maximum during the time that the transmitted action potential reaches the other end, and finally returning once more to zero after it. The time delay of such action potentials through the stopper indicated propagation velocities of about 0.15 cm · sec^{-1} in the stopper.

Measurements were also made of such volume flows during a small net osmotic volume flow of 0.89 nliter · sec^{-1} (about twice the maximum velocity of the action potential volume flow rate). The object of this experiment was to determine if there was any significant change in L_p during excitation. The results indicated that there was not.

the volume flow rate with that of the potential changes during the action potential

p.d., E_R (mV)	Measured volume flows (divided by cell area A) per unit area		Fully corrected volume flow rate per unit area	$e^{-EF/RT}$
	$\Delta V_m/A$ (nliter · cm^{-2})	$(dV/dt)_m/A$ (nliter · sec^{-1} · cm^{-2})	$(dV/dt)_m/A$ [e] (nliter · sec^{-1} · cm^{-2})	
171 ± 1	0.67 ± 0.05	0.36 ± 0.04	0.80 ± 0.09	837
172 ± 3(11)	0.79 ± 0.08	0.34 ± 0.04	0.78 ± 0.09	871
193 ± 2	3.38 ± 0.50	0.50 ± 0.12	1.22 ± 0.29	1,980
145 ± 6	0.50 ± 0.06	0.32 ± 0.02	0.73 ± 0.04	299
173 ± 3	1.34 ± 0.68	0.38 ± 0.04	0.88 ± 0.11	907

[e] Fully corrected for the transcellular method of measurement, the fraction of the cell in the split-stopper (both from Eq. (25) in paper II), and for the time delay of the chart recorder (0.12 sec; obtained from Eq. (48) in paper II).

[f] Errors shown are the SEM.

[g] Simple averages over all the cells except for $\tau_v - \tau_{ap}$ where they are the weighted means and virtually represent the mean and SEM of all individual measurements used.

Table 1 summarizes all the measurements. The average maximum rate of volume flow per unit area of cell membrane surface during an action potential was 0.88 ± 0.11 nliter · sec^{-1} · cm^{-2} in the direction of an outflow from the cell. As mentioned in the table legend, this value has been fully corrected for the transcellular method of measurement, the fraction of cell in the stopper, and the time constant of the chart recorder. These corrections are discussed in detail in II where it is shown, for example, that the actual volume outflow at one end of a cell is about twice the transcellular volume flow measured. Similarly, the corrected total volume of solute and water leaving a cell during excitation would be just over twice the measured value of 1.34 nliter · cm^{-2}.

The membrane potential is directly related to the concentrations immediately adjacent to it $\left(\text{if } P_{Cl}/P_K = 0,\ E \simeq -(RT/F) \ln \left\{\frac{P_K[K]_i + P_{Na}[Na]_i}{P_K[K]_o + P_{Na}[Na]_o}\right\}\right)$ and thus can be a measure of the solute driving force across the membrane. Therefore, it might be expected that the flux of solute during an action potential, and consequently also the volume flow, would be related to the membrane resting potential. In fact there is quite a good correlation (correlation coefficient = 0.97) between the values of $(dV/dt)_m/A$ and $e^{-EF/RT}$ given in Table 1. In these experiments, it should also be noted, that the

ratio of the peak change in potential ΔE to the resting potential E_R was 0.88 ± 0.04.

Also, the time course of the volume flow rate follows the change in cellular potential quite closely, the maximum rate lagging slightly behind the peak of the action potential by 0.17 ± 0.08 sec.

Pressure Changes

There were pressure changes during an action potential which corresponded to a drop in pressure of the cell's interior during excitation. This is illustrated in Fig. 9 for two different cells. As shown in this figure, two main types of response were observed. In some cases such as action potential 6F-1, there was a decrease in pressure during the action potential and no immediate recovery, whereas in action potential 6N-7 the decrease was followed by a slow recovery to its initial resting value.

The rates of change of pressure were reconstructed from the recorder charts, and two examples are shown uncorrected for time delays in Fig. 10 for cell 6N.

The corrected values of all results are shown in Table 2. The average maximum decrease in pressure ΔP_m was $19.3 \pm 2.9 \times 10^{-3}$ atm, and the

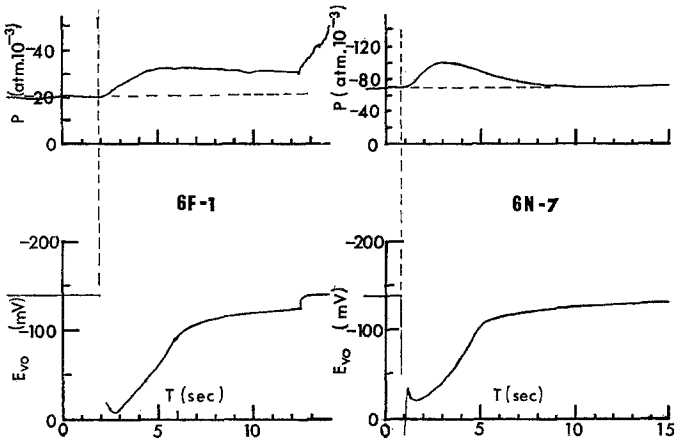

Fig. 9. Fast recording of the typical changes in pressure P (atm$\times 10^{-3}$) and membrane p.d., E_{V0}, during an action potential for three cells of *Chara australis*. For run 1, cell 6F was in a solution of A.P.W. (1.0). This recording shows the decrease in pressure with no recovery back to the original pressure. For run 7, cell 6N was in a solution of A.P.W. (0.2). This recording shows the other type of response in which the pressure recovers completely shortly after the action potential. In this particular case, the moment of inertia of the recording system had been increased from about 990 to 1465 g·cm^2. In each case, as discussed in the text, the time constant of the measuring circuit was about 0.27 sec

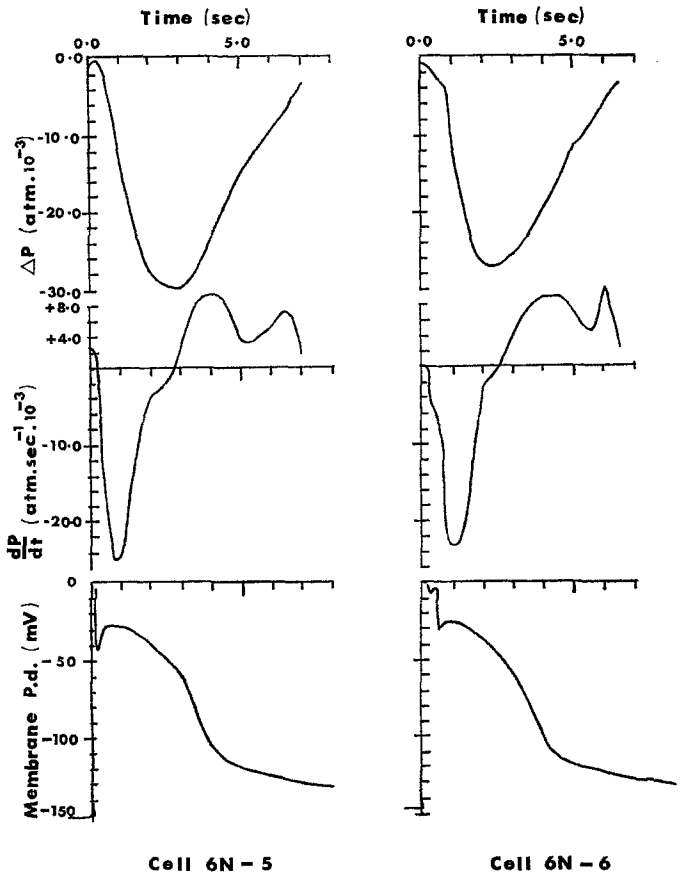

Fig. 10. Typical changes in pressure, ΔP (atm$\times 10^{-3}$), rate of change of pressure, dP/dt (atm$\cdot$sec$^{-1}\times 10^{-3}$) and membrane p.d., E_{V0} (mV) for a cell of *Chara australis* (cell 6N) in A.P.W. (0.2). Runs 6N-5 and 6N-6 were measured using the "knife-edge" and "round" bearing, respectively

average maximum rate of change of pressure $(dP/dt)_m$ was $19.6\pm3.8\times10^{-3}$ atm $\cdot$ sec^{-1}. There seemed to be no correlation between the pressure changes and any simple function of the cells' resting potential E_R or change in potential ΔE. In these experiments, the average ratio $\Delta E/E_R$ was 0.88 ± 0.06.

Again the time course of the rate of change of pressure followed the change in cellular potential closely, this time with the maximum rate leading the peak of the action potential by 0.09 ± 0.07 sec.

It was noticed that for some cells, when conditions were either less suited to total initial excitation of the whole cell or more suited to a slower propagation velocity, the time delay $(\tau_p-\tau_{ap})$ had increased. For example, when the current was lowered to 75% of its previous value and cell 6G,

Table 2. *Corrected pressure changes, rate of change of pressure and correlation of the time for the latter to reach a maximum, τ_p, with the time taken for the action potential to reach a maximum, τ_{ap}*

Exp.	No. of action potentials used	α	Cell length (cm)	Cell radius (mm)	Time constants (sec)		p.d., E_R (mV)	Pressure changes [a]	
					τ_{ap}	$\tau_p - \tau_{ap}$		$\Delta P'_m$ (atm $\times 10^{-3}$)	$(dP/dt)'_m$ (atm sec$^{-1} \times 10^{-3}$)
6 F 1–6	4	0.90	3.1	0.505	0.74 ± 0.03 [b]	-0.16 ± 0.06	141 ± 2	11.7 ± 1.8	11.3 ± 0.8
6 G 1–6	4	0.48	1.8	0.50	0.68 ± 0.10	0.16 ± 0.15	178 ± 6	14.7 ± 0.9	15.0 ± 3.7
6 J 3	1	0.47	6.7	0.444	1.22	-0.29	175	12.4	19.7
6 K 1–6	6	0.48	4.5	0.60	2.08 ± 0.24	$+0.75 \pm 0.23$	189 ± 9	31.5 ± 6.5	15.4 ± 3.6
6 M 2–10	6	1.63	1.76	0.563	0.96 ± 0.05	-0.21 ± 0.04	139 ± 2	22.7 ± 2.5	31.5 ± 2.7
6 N 1–8	6	0.37	1.8	0.51	0.69 ± 0.02	-0.16 ± 0.02	147 ± 3	26.3 ± 2.6	35.6 ± 4.2
6 N 10–18	8	0.43	1.8	0.51	2.08 ± 0.02	-0.63 ± 0.05	107 ± 2	16.1 ± 1.8	8.8 ± 0.05
Average values of parameters [c]						-0.09 ± 0.07	147 ± 5	19.3 ± 2.9	19.6 ± 3.8

[a] Both the magnitudes and time courses of the pressure changes and the rates of change of pressure have been corrected for the time delay of the chart recorder (0.12 sec) and of the filter circuit (0.27 sec). These corrections have been analyzed in detail in paper II and have been calculated using Eq. (48) in that paper.

[b] Errors shown are the SEM.

[c] Simple averages over all the cells in each case, except for $\tau_p - \tau_{ap}$ where they are the weighted means and virtually represent the mean and SEM of all individual measurements used.

was just stimulated, the time delay increased from 0.46 ± 0.14 sec (four measurements) to 1.68 sec (one measurement, 6G-2). For cell 6M, the difference in time delays in A.P.W. (0.1) when the cell was stimulated with a current of 2 and 6 μamp was 0.16 sec (6M-2 and 6M-3, one measurement each only). Again for cell 6N, when the cell was stimulated (6N-4), only 250 sec after the previous stimulation the delay changed from -0.01 ± 0.02 to $+0.34$ sec.

Also of some interest was the change in pressure recorded while both internal KCl-filled glass microelectrodes (about 10 to 20-μ tip diameter) were being inserted into the cell. The pressure dropped about 0.1 atm during insertion of the electrodes.

Discussion

Thus both volume flows and pressure changes have been measured during an action potential in cells of *Chara australis*. The volume flow rates in an outflow direction were about 0.88 ± 0.11 nliter $\cdot$ sec$^{-1} \cdot$ cm^{-2}, and the rates of change of pressure (the pressure dropping) were about $19.6 \pm 3.8 \times 10^{-3}$ atm $\cdot$ sec^{-1}. (The maximum drop in pressure was $19.3 \pm 2.9 \times 10^{-3}$ atm, representing a 0.3% change in cell pressure.) Both changes follow the action potential quite closely, the maximum volume flow rate appearing to lag just behind the peak of the action potential by 0.17 ± 0.08 sec and the maximum rate of pressure change leading it by 0.09 ± 0.07 sec.

One important factor affecting the time course of flows and pressure changes which has already been mentioned is the effect of the cell being only partially excited initially. For example, it is shown in Appendix C that the time delays for peak volume flow, or rate of pressure change, when the central half of the half length of the cell, the end half, just the center or the end of the cell is excited initially, are given by $\ell/16V$, $\ell/4V$, $\ell/8V$ and $\ell/2V$, respectively (where ℓ is the half length of the cell in the volume flow experiments and the whole length in the pressure ones, and V is the propagation velocity of the cell action potential). Thus for a propagation velocity greater than 8 to 16 cm $\cdot$ sec^{-1}, the peak volume flow rate would be retarded by less than 0.03 or 0.06 sec when the central or end 2-cm^2 portion only of a cell of 4-cm half length was stimulated initially. This might increase to 0.06 and

2 The currents used were normally at least 50% greater than the threshold values for excitation and for an A.P.W. (0.5) medium; the space constant was estimated to be about 0.9 cm. Thus a current electrode centrally placed at one end of the cell could be expected to stimulate initially almost 2 cm of the cell.

0.12 sec if the cell was stimulated only at the middle or at one end, and may be partly the explanation of the very slight delay of 0.17 ± 0.08 sec observed. Similarly, in the pressure experiments with the much smaller cells, a 2-cm cell stimulated only at one end would cause the peak rate of change of pressure to be retarded by only about 0.06 to 0.1 sec, and proportionately longer for longer cells (although the internal electrodes were never placed further than about 1.5 cm from the center of the cell). In these pressure measurements, such time delays were probably negligible. Further discussions of these results will be continued in paper II, where the mechanisms underlying the volume flow and the relationships between the volume flows and pressure changes during an action potential will be analyzed in detail.

Volume flows have also been measured for another *Characean* cell, *Nitella flexilis*. Fensom (1966) in his preliminary measurements reported water flows of 0.2 nliter per action potential which followed the action potential quite closely. These, however, were not corrected for the transcellular nature of his experimental arrangement. Such corrections can be estimated and would result in flows of about 0.9 nliter $\cdot$ sec^{-1} $\cdot$ cm^{-2} (using an estimated cell half area of about 0.5 cm^2) which are comparable with the values reported in this paper. Kishimoto and Ohkawa (1966), however, observed much smaller flows for *Nitella flexilis* of about 0.07 nliter $\cdot$ cm^{-2}. In contrast to the measurements reported in this paper and those of Fensom (1966), which indicated that the volume flow followed the action potential very closely (*see* Fig. 6), Kishimoto and Ohkawa (1966) found a delay of about 2 sec between the peak of the action potential and the waterflow. Both this time lag and the very low magnitude of their flows (approximately 1/10 of the magnitude of those obtained by this author for *Chara* and Fensom for *Nitella*) suggests that the inertia of their measuring system was a limiting factor in their experiments. In other words, the results of Kishimoto and Ohkawa (1966) would be quite compatible with the results in this paper if their recording system had a time constant of about 5 sec since this would result in a time delay approximately given by $\theta = \tan^{-1} \omega\tau_2$ and a reduction factor given by $\cos\theta = 1/(1-[\omega\tau_2]^2)^{1/2}$ (as indicated by Eq. (48) in II) where ω is the radial frequency of the action potential and τ_2 is the time constant of the recording or measuring circuit.

I am indebted to Professor A. B. Hope, my former Ph. D. supervisor, for helpful advice and encouragement during this work. I would also like to thank Drs. J. Dainty, R. S. Eisenberg and E. M. Wright for their helpful critical readings of the manuscript.

I was the holder of research studentships from the Australian Commonwealth Scientific and Industrial Research Organization and Flinders University during the

course of most of this work, which was carried out at both the University of Sydney and Flinders University, and is included in part III of my Ph. D. thesis (Barry, 1967). The work was also supported in part at the University of California at Los Angeles by Public Health Service grant GM 14772.

Appendix A

An Outline of the Method Used to Derive the Theoretical Relationship Between the Deflection of a Wedge Resting Transversely Across a Cell and the Turgor Pressure of the Cell

The relationship between the two parameters was derived theoretically by considering the equilibrium situation obtained when the following two conditions are satisfied. (1) The net force acting on the wedge must be zero (i.e., the weight of the wedge must be supported by the vertical components of the tension in the cell wall). (2) The work done by the wedge in causing the deflection of the cell wall must equal the increase in elastic potential energy of the wall. This latter is equal to the work done against the elastic tension in increasing the surface area of the cell wall both longitudinally and laterally.

In order to calculate this change in surface area, four more conditions were assumed: (1) that the cell will deform in such a way that its volume will remain constant; (2) that its lateral bulging will be such that its circumference will tend to remain circular and of just slightly smaller radius of curvature than that of the original cell; (3) that the tension in the cell wall and the pressure in the cell will not be significantly changed by the deformation; and (4) that the deflection will be small enough so that a considerable number of approximations may be made concerning angles and their circular functions.

It may then be shown that

$$P=\alpha\frac{Mg}{aX}$$

where P is the cell's turgor pressure, Mg is the weight acting through the wedge, a is the cell radius, X is the deflection and α is a constant of the deformation $\simeq\sqrt{5/32}\simeq 0.4$.

Full details of the analysis have been given (Barry, 1967) and will be published subsequently.

Appendix B

Investigations of the Time Response of the Pressure Transducer

The theoretical response of the transducer arrangement was investigated (Barry, 1967), and it was calculated that for pressure changes occurring in times greater than about 10 msec the moment of inertia of the measuring system has a negligible effect on the time course of the deflection. This is supported by the following experimental evidence that both extra inertia and the increased area of bearing surfaces do not cause any significant increase in the time delays. For these experiments the relative time delays were measured for the two different fulcrum-bearing surfaces, discussed earlier (p. 319). For cell 6N, both the round and knife-edge surfaces were used. In the case of the round bearing surface, the delay of the action potential peak from the maximum rate of change of pressure ($\tau_{pm}-\tau_{ap}$) was -0.01 ± 0.02 sec (average of three measurements) whereas the knife-edge apparently caused an *increase* to 0.06 ± 0.02 sec (two measurements).

The effect of inertia was also investigated with the same cell using the round bearing surface. Increasing the moment of inertia of the measuring system from about 990 (three measurements) to 1,465 g·cm^2 (two measurements), the time delay difference was only 0.05 ± 0.04 sec.

The magnitudes of the maximum rate of pressure change were 21 ± 5, 27 ± 1 and $32 \pm 5 \times 10^{-3}$ atm·sec^{-1} for 'round' bearings with normal inertia, increased inertia and 'knife-edge' bearings with normal inertia, respectively.

In each of the above cases, the errors shown are the approximate SEM.

Appendix C

To Determine the Effect of Action Potential Propagation on Retardation of Overall Volume Flows and Pressure Changes for a Cell Which is Only Partially Excited Initially

Case 1. Consider a cell of length ℓ being stimulated only at its center. If the flow per unit area during an action potential is given by the function $j(t)$, which is a sectionally smooth continuous function (i.e., mathematically 'well behaved', differentiable, etc.) of time with no discontinuities, then it may be represented by a Fourier series (Courant, 1937, pp. 439, 447). In fact most of the contribution would come from a harmonic of frequency ω, where $\omega = \pi/\tau_m$, τ_m being the time taken for the flow to reach a maximum. Now the action potential and presumably any volume flow resulting from it is in the form of a single waveform defined well, for example, for $0 \leqq t \leqq 4\,\tau_m$. However, as discussed in Courant (1937, p. 426), one can arbitrarily extend such a function as a periodic one, in this case most simply as an odd function of period $4\,\tau_m$ provided, of course, that in any later calculations one does not make use of any contributions of the extended function outside of the well-defined interval ($0 \leqq t \leqq 4\,\tau_m$). In this, case because it is an odd function, the action potential may be represented as a sine series (Courant, 1937, p. 440) and hence the total flow per unit area may be written as

$$j(t) = \sum_{n=0}^{n=\infty} j_{n\omega} \sin n\omega t .$$

For notation convenience n will be dropped so that $j(t)$ will be written as

$$j(t) = \sum_{0}^{\infty} j_{\omega} \sin \omega t \tag{C.1}$$

where $j(t) = 0$ when $t = 0$.

Consider the x axis as along the length of the cell with $x = 0$ at the center. After the cell has been stimulated at $x = 0$, the action potential flow at any point x will be given by

$$j(t, x) = \sum_{0}^{\infty} j_{\omega} \sin \omega \left(t - \frac{x}{V}\right) \tag{C.2}$$

where V is the propagation velocity of the action potential along the cell. Hence the average volume flow/unit area, $\overline{j(t)}$, is given by

$$\overline{j(t)} = \frac{2 \int_{0}^{\ell/2} 2\pi a \sum_{0}^{\infty} j_{\omega} \sin \omega \left(t - \frac{x}{V}\right) dx}{2\pi a \ell} \tag{C.3}$$

i.e.,

$$\overline{j(t)}=\frac{2}{\ell}\left[\sum_0^\infty j_\omega \frac{V}{\omega}\cos\omega\left(t-\frac{x}{V}\right)\right]_0^{\ell/2}$$
$$=\frac{2}{\ell}\sum j_\omega \frac{2V}{\omega}\sin\frac{\ell\omega}{4V}\sin\omega\left(t-\frac{\ell}{4V}\right). \tag{C.4}$$

When $\frac{\ell\omega}{2V}$ is small (i.e., $\leqq 0.1$), Eq. (C.4) becomes

$$\overline{j(t)}=\sum_0^\infty j_\omega \sin\omega\left(t-\frac{\ell}{4V}\right). \tag{C.5}$$

This implies that the average of each Fourier component is retarded by $\ell/4V$ seconds independent of its frequency, and so the average of the flow owing to the whole action potential must be retarded by $\ell/4V$ seconds.

Case 2. Assume that the same situation applies as in case 1 except that the middle half of the cell is stimulated initially, from $x=\frac{-\ell}{2}$ to $\frac{+\ell}{2}$.

Then

$$\overline{j(t)}=\frac{4\pi a\left[\left\{\int_0^{\ell/4}\sum_0^\infty j_\omega \sin\omega_{\dot{x}}\left(t-\frac{x}{V}\right)dx\right\}+\sum_0^\infty j_\omega\left(\frac{\ell}{4}\sin\omega t\right)\right]}{2\pi a\ell}. \tag{C.6}$$

If $\frac{\omega\ell}{8V}$ now $\lesssim 0.1$ as before,

$$\overline{j(t)}=\frac{2}{\ell}\left[\sum\left\{\frac{\ell}{4}j_\omega\sin\omega\left(t-\frac{\ell}{8V}\right)+j_\omega\frac{\ell}{4}\sin\omega t\right\}\right], \tag{C.7}$$

$$\overline{j(t)}=\sum_0^\infty j_\omega\sin\omega\left(t-\frac{\ell}{16V}\right)\cos\frac{\omega\ell}{16V}. \tag{C.8}$$

But $\frac{\omega\ell}{16V}\ll 0.1$ if $\frac{\omega\ell}{8V}\lesssim 0.1$; hence,

$$\overline{j(t)}=\sum_0^\infty j_\omega\sin\omega\left(t-\frac{\ell}{16V}\right). \tag{C.9}$$

As before, the average flow produced by the whole action potential is now retarded by $\ell/16V$.

Case 3. Assume that the same situation applies as in case 1 except that just one end of the cell is stimulated, at $x=-\ell/2$.

This case is equivalent to case 1 except that ℓ is doubled; i.e.,

$$\overline{j(t)}=\sum_0^\infty j_\omega\sin\omega\left(t-\frac{\ell}{2V}\right) \tag{C.10}$$

provided that $\frac{\omega\ell}{2V}\lesssim 0.1$ and so the retardation is $\ell/2V$.

Case 4. Assume that the same situation applies as in case 1 except that one end half of the cell is stimulated initially, from $x=0$ to $\ell/2$.

This case is again equivalent to case 2 except that ℓ is doubled; i.e.,

$$\overline{j(t)}=\sum_{0}^{\infty} j_{\omega} \sin \omega \left(t-\frac{\ell}{8V}\right) \tag{C.11}$$

provided that $\frac{\omega \ell}{4V} \lesssim 0.1$.

Thus, for these four cases, provided the propagation velocity is sufficiently fast, the overall flow is not affected significantly in magnitude and is merely retarded by the factors $\ell/4V$, $\ell/16V$, $\ell/2V$ and $\ell/8V$ for the cases in order.

References

Barry, P. H. 1967. Investigation of the movement of water and ions in plant cell membranes. Ph. D. Thesis. University of Sydney, Sydney, Australia.

— 1970. Volume flows and pressure changes during an action potential in cells of *Chara australis*. II. Theoretical considerations. *J. Membrane Biol.* **3**:335.

— Hope, A. B. 1969. Electro-osmosis in membranes: Effects of unstirred layers and transport numbers. Part II. Experimental. *Biophys. J.* **9**:729.

Courant, R. 1937. Differential and Integral Calculus, Vol. I. (2nd Ed.). Blackie and Sons Ltd, London and Glasgow.

Fensom, D. S. 1966. Action potentials and associated waterflows in living *Nitella*. *Canad. J. Botany* **44**:1432.

Kishimoto, U., Ohkawa, T. 1966. Shortening of *Nitella* internode during excitation. *Plant Cell Physiol.* **7**:493.

Kobatake, Y., Fujita, O. 1964*a*. Flows through charged membranes. I. Flipflop current vs. voltage relation. *J. Chem. Phys.* **40**:2212.

— — 1964*b*. Flows through charged membranes. II. Oscillation phenomena. *J. Chem. Phys.* **40**:2219.

Tazawa, M. 1957. Neue Methode zur Messung des Osmotischen Wertes einer Zelle. *Protoplasma* **48**:342.

Teorell, T. 1958. Transport processes in membranes in relation to the nerve mechanism. *Exp. Cell Res.* **5**:83.

— 1961. An analysis of the current-voltage relationship in excitable *Nitella* cells. *Acta Physiol. Scand.* **53**:1.